

SYNCHRONOUS PHASE AND ENERGY MEASUREMENT SYSTEM FOR A 6.7-MeV H⁻ BEAM*

J. D. Gilpatrick, R. E. Meyer, F. D. Wells, J. F. Power, R. E. Shafer
MS-H808, Los Alamos National Laboratory, Los Alamos, NM 87545

Abstract

A noninterceptive measurement system has been built to measure the energy and synchronous phase of a 6.7-MeV proton beam drifting from the ramped-gradient, drift-tube linac (RGDTL) in the accelerator test stand (ATS) facility. Axially-symmetric, capacitive probes used in these measurements produce signals that are proportional to the beam image current on their inner rings. Signals from two of these probes separated by 92.6 cm are down-converted from 425 to 20 MHz. The phase difference between these 20-MHz signals is then detected with an electronic, phase-comparator circuit. The phase-comparator signal output is a voltage that is related to momentum of the beam. A phase comparison is also provided between the 425-MHz fundamental RF field inside the RGDTL and the capacitive probe located nearest the RGDTL output. The total estimated error for the absolute and relative energy measurement is less than ± 12.2 and ± 3.1 keV, respectively. The total estimated error for the relative synchronous phase measurement is less than $\pm 1^\circ$. Beam energy versus synchronous phase experimental data agree with computer simulations.

Introduction

To test the RGDTL, the ATS at Los Alamos National Laboratory required an on-line, noninterceptive measurement of beam energy and synchronous phase. These on-line measurements operate with a beam current of 10 to 100 mA of an H⁻ beam. The accelerator typically runs at a 5-Hz rate and has a 50 μ s-long macropulse. The block diagram in Fig. 1 shows the main components of this

system. These components are the three capacitive probes installed on the ATS beamline, the rf field loop inside the RGDTL, a down-converter chassis that consists of four conversion channels, and a phase-comparator chassis that consists of three output comparison channels. These three output channels provide an approximate energy, a more accurate energy, and a relative synchronous phase measurement.

Capacitive Probes and Their Placement

Figure 2 shows capacitive probe #1 that is installed in the ATS beamline. The stainless steel support structure attached to the beamline grounds the outer ring, and the vacuum-sealed, coaxial-connector's inner conductor is attached to the inner concentric ring. This first probe assembly is contained within a 2.5-cm-thick, beampipe flange attached to the outer bulkhead flange of the RGDTL and does not interfere with other accelerator and beamline components. Probes #2 and #3 are mounted on a short section of flanged beam pipe that is installed in the ATS beamline as a self-contained unit.

Probe #1 is located 11.1-cm downstream from the RGDTL final drift tube. The 92.6-cm drift distance between probe #1 and probe #3 is chosen to ensure an energy measurement accuracy of $\pm 0.2\%$. Because there can be 10, 11, or 12 bunches between probes #1 and #3, the 8.4-cm distance between probes #2 and #3 verifies the more accurate measurement by identifying the correct integer number of bunches. A 3/8-in. phase-stabilized, coaxial cable that is electrically tuned to within $\pm 0.5^\circ$ of phase at 425 MHz, using coaxial line stretchers, transports each signal to the electronics.

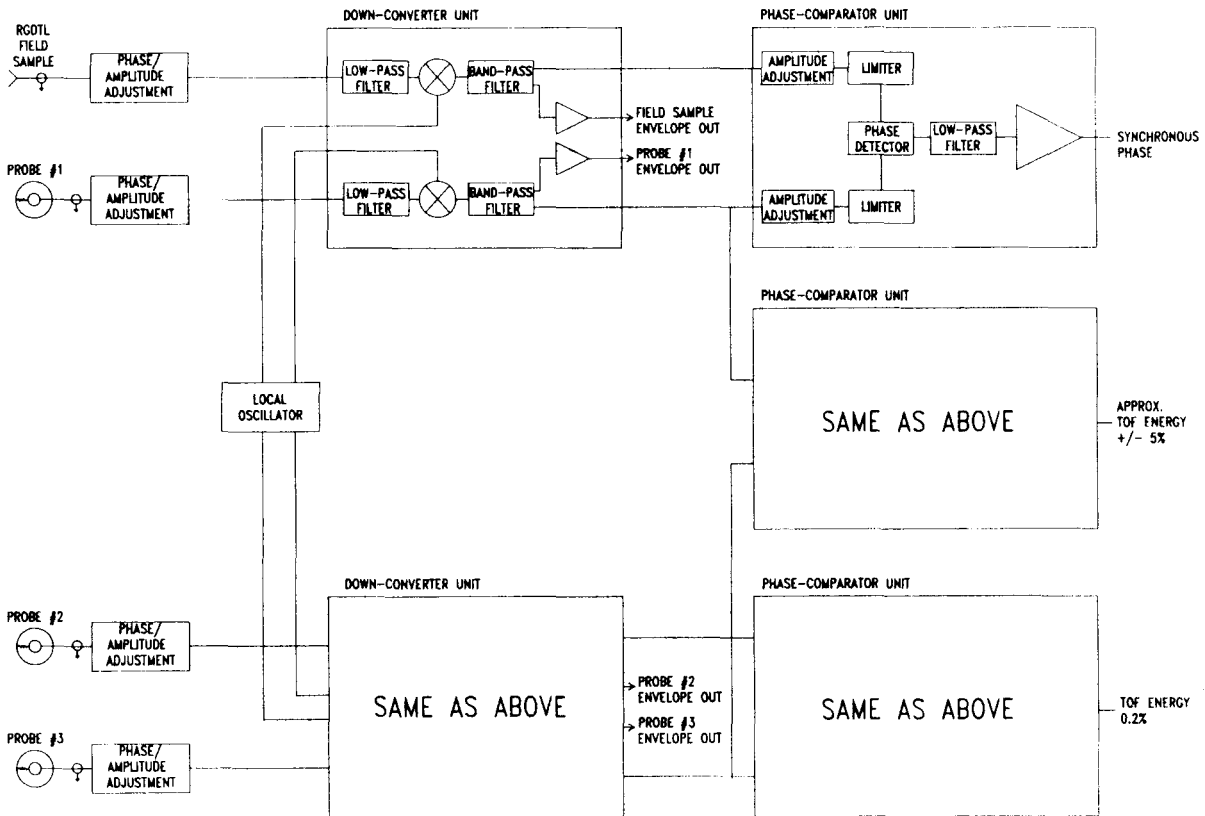


Fig. 1. The system block diagram shows the key components of the down-conversion and phase-comparator units.

*Work supported and funded by the US Department of Defense, Army Strategic Defense Command, under the auspices of the US Department of Energy.



Fig. 2. The concentric inner and outer rings of capacitive probe #1 are connected to a 50- Ω back-termination resistor and a SMA coaxial connector.

Estimates of the probe signals were made using a simple mathematical model that combines the beam image currents of the bunched beam (typical bunch length of 1.9 mm rms) with the probe as a single-pole filter.^{2,3} The analytic description of the coupling impedance Z_0 is then given by

$$Z_0(\omega) = \frac{\omega \ell R}{\beta c} \frac{\omega R C_p + j}{\left[(\omega R C_p)^2 + 1 \right]} \quad (1)$$

where R is the terminating resistance, C_p is the probe capacitance (about 2pF), βc is the beam velocity, ℓ is the inner ring length, and ω is the frequency. Half of the signal power flows to the 50- Ω terminating resistor on the probe and the other half flows to the electronics through the cable. The power presented to the coaxial cable is

$$P(\omega) = \frac{Z_o^2(\omega)}{Z_c} \langle I_b \rangle^2 \quad (2)$$

where Z_c is the characteristic impedance and equals R , and $\langle I_b \rangle$ is the average beam current.

The probe's specifications and signals are summarized in Table I below

TABLE I. PROBE GEOMETRY

Probe	Beam Aperture (cm)	Inner Ring Aperture (cm)	Inner Ring Length (cm)	Beam Width (cm) (4σ)	Expected Signal Power (dBm) $\langle I_b \rangle = 10$ mA
#1	1.0	1.2	0.5	0.25	2.5
#2	3.4	3.6	0.5	1.50	1.5
#3	3.4	3.6	0.5	1.60	1.5

Down-Converter Chassis

The down converter chassis uses double-balanced mixers to convert each incoming 425-MHz signal to a 20-MHz intermediate-frequency (IF) signal. The output power of the mixer is expressed as

$$P \propto \frac{V_{in} V_{\ell o}}{2} \cos \left((2\pi(f_{in} - f_{\ell o})t + \phi_{in}) \right) \quad (3)$$

where $f_{\ell o}$ is the local oscillator frequency, f_{in} is the fundamental component of each probe's radio-frequency (RF) signal, and ϕ_{in} is the phase of the incoming signal. The phase of the input RF signal is preserved in the output IF signal of the mixer.

Each of the four channels in the down-converter chassis consists of a set of line stretchers and an adjustable attenuator used to equalize the channel phase and amplitude, an amplifier/low-pass filter to select only the 425-MHz fundamental component, a double-balanced mixer, a band-pass filter to eliminate higher mixed frequencies, and some final buffering amplifiers. The attenuation through a coaxial cable and mixer channel is 1.9 and 16.8 dB, respectively.

Phase-Detection Chassis

As the block diagram shows, the power of the four incoming down-converted signals is divided and adjusted for the three specific measurements—the approximate energy, the more accurate energy, and the synchronous phase. These signals are then limited with a pair of high-gain comparators that convert each analog signal to a digital signal with the same input phase. Two separate digital signals are compared using an RS flip-flop phase comparator whose output voltage level is a 20-MHz pulse train with a duty factor, DF , such that

$$DF = \frac{\phi_1 - \phi_2}{2\pi}; \quad \phi_1 = \pi, -\pi \leq \phi_2 \leq \pi \quad (4)$$

where ϕ_1 and ϕ_2 are the incoming signal phases. The output signal is then filtered and amplified to set the conversion factor to 72° per volt.

For the energy measurement where the probe signals are compared over the dynamic range of the beam current, the limiter pair must preserve the same input phase difference. In the case of the synchronous phase measurement, the RF field sample signal does not vary by more than ± 1 dB, whereas probe signals may vary by as much as 20 dB. The selected set of limiters has a 20-dB window within its limiting dynamic range whereby the input-to-output phase varies by only $\pm 0.5^\circ$ at 20 MHz.

The Motorola MC 12040 phase comparator chip chosen has the required accuracy, but has a range of $\pm 2\pi$. This is twice as much as is needed; therefore, an ambiguity in the measurement is present. Because there are two sets of outputs from the phase detector chip, the U and \bar{U} set of outputs are used to feed the differential input of an operational amplifier. There are input signal phase conditions that will produce an accurate signal on one output pair, but can cause one or both of the other output pair to swing to the emitter-coupled logic supply voltages. To avoid these inaccurate conditions, the range of measured input phase difference must be limited to less than $\pm 0.9\pi$. An improved version of the phase detector that has an unambiguous $\pm \pi$ phase angle range is currently being designed.

The errors in these measurements are primarily due to two major contributors: the accuracy to which the distance between probes is measured and the accuracy to which the 20-MHz phase differences are measured. The absolute phase error was estimated to within $\pm 3.6^\circ$ at 425 MHz, and the resolution of the phase measurement was $\pm 1^\circ$, which corresponds to an energy measurement absolute accuracy and resolution of ± 12.2 and 3.1 keV. Because the electrical length of the coaxial cable for the RGDTL field monitor is not measured, the absolute phase is unknown but the relative synchronous phase is resolved to within $\pm 1^\circ$. The synchronous phase and energy measurements have an overall bandwidth of 2 MHz.

RGDTL Measurement Application

The specific measurement is a series of energy and synchronous phase measurements as the RGDTL rf power and input phase are varied. The 20-MHz phase data are acquired from the system outputs of synchronous phase and energy channels. They are then converted to time and

transformed to energy E and synchronous phase ϕ_s , using the relations:

$$E = Mc^2 \left\{ \left[1 - \left(\frac{L}{c \left(nT + \left(\tau_{IF} T_{IF} \right) \right)} \right)^2 \right]^{1/2} \right\} \quad (5)$$

and

$$\phi_s = \phi_{fs} - \phi_1 - 360^\circ \left(\frac{z_s}{\beta \gamma} \right) \quad (6)$$

where τ_{IF} is the measured time; T_{IF} is the IF period; T is the RF period; L is the drift distance between probes #1 and #3; n is the number of integer $\beta\gamma$ in L; Mc^2 is the rest energy of the particles; ϕ_{fs} and ϕ_1 are the measured phases of the rf field sample and probe #1, respectively; and z_s is the drift distance between probe #1 and the last accelerating gap. Figure 3 shows the experimental data and computer simulations of beam energy versus synchronous phase.

Conclusion

This measurement technique can be included with the standard position-monitor system so that six centroids, four transverse and two longitudinal, can be obtained without intercepting the beam or impairing the accelerator operation. Standard position and intensity measurements will be integrated into the next upgrade of this measurement system.

Measuring the down-converted phase with digital techniques provides a $\pm 1^\circ$ RF phase resolution and a $\pm 0.9n$ phase range over a 20-dB dynamic range. With the proper choice of electronic components and circuit design, one should be able to remove the phase ambiguity while increasing the dynamic range to 40 dB.

Acknowledgments

The authors would like to acknowledge the efforts of Paul Carrier, Lee Johnson, Robert Runyon, Stephen Shurtleff, Brad Shurter, Laybe Torres, and Joseph Uher without whom these measurements would not have existed. Also, we appreciated the conversations with Kenneth Johnson and Oscar Sander of the ATS experimental team.

References

1. J.D. Gilpatrick and D.D. Chamberlin, "FMIT Diagnostics Instrumentation," IEEE Trans. Nucl. Sci. 32 (5), 1962 (1985).
2. R. E. Shafer, "Characteristics of Directional Coupler Beam Position Monitors," IEEE Trans. Nucl. Sci. 32 (5), 1933 (1985).
3. T. Linnecar, "The High Frequency Longitudinal and Transverse Pick-ups used in the SPS," CERN-SPS/ARF/78-17, CERN PUBLICATION.

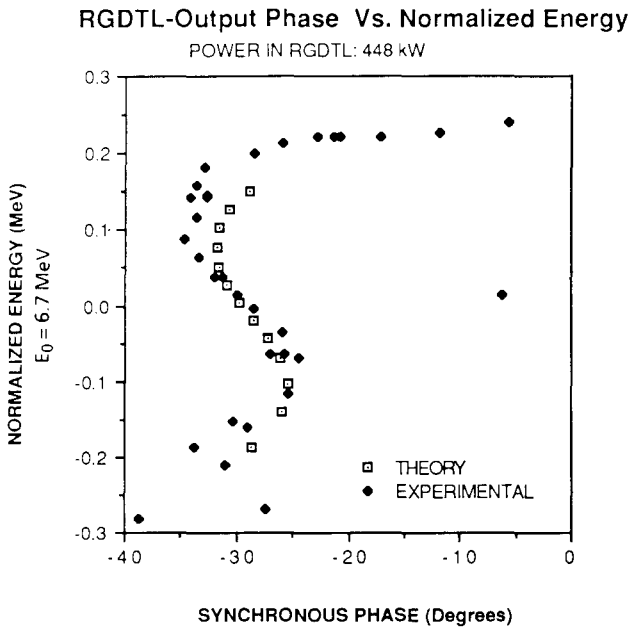


Fig. 3. The measured synchronous phase versus energy data and computer simulations for the RGDTL.